

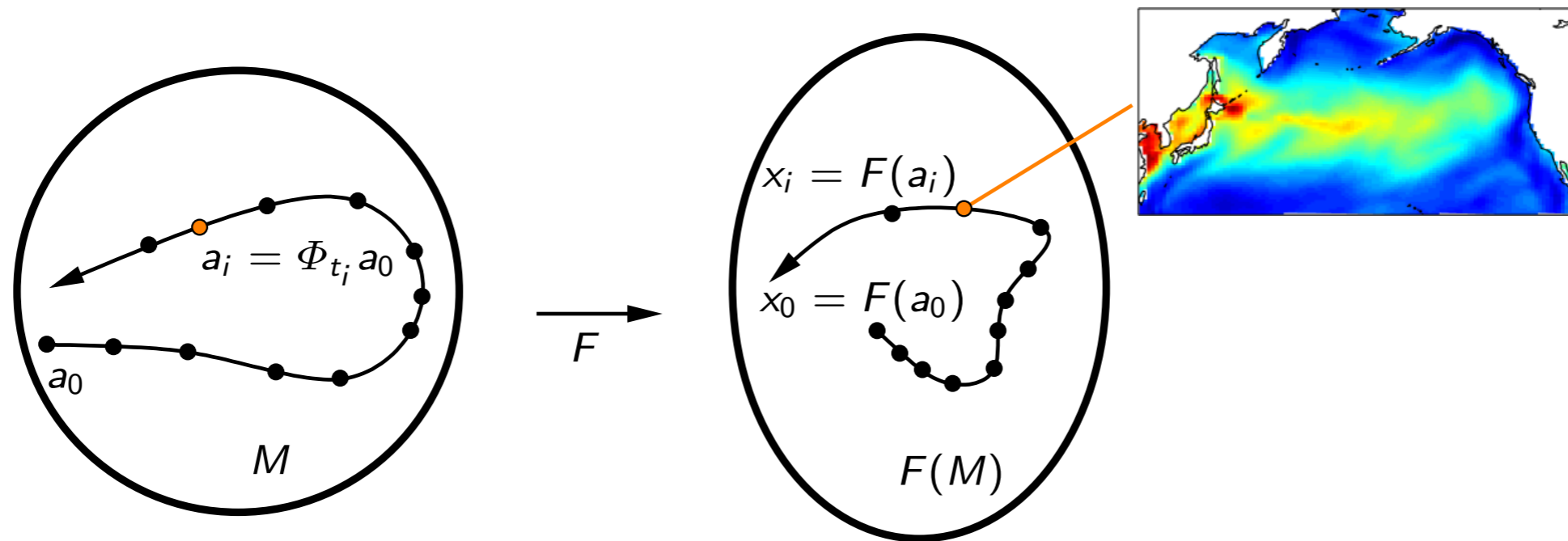
Recovering spatiotemporal modes of variability
in the ocean and atmosphere
using kernel and Koopman operators

Joanna Slawinska¹ & Dimitris Giannakis²

¹Center for Environmental Prediction, Rutgers University

²Courant Institute of Mathematical Sciences, NYU

Setting



Ergodic dynamical system (M, Φ_t, μ) observed through a vector-valued function $F : M \mapsto \mathbb{R}^n$

Given time-ordered observations $\{x_0, \dots, x_{N-1}\}$ with $x_i = F(a_i)$ and $n \gg 1$, we seek to compute approximate Koopman eigenfunctions with high smoothness

Kernel methods for Koopman eigenfunctions (Giannakis 2015, Giannakis et al. 2015)

We formulate a Galerkin method for the Koopman eigenvalue problem in a data-driven basis of $L^2(M, \mu)$ with a well-defined notion of smoothness (Dirichlet energy)

- Takens delay embeddings

$$F_s : M \rightarrow \mathbb{R}^{sd}, \quad F_s(a) = X = (F(a), F(\Phi_{-\delta t} a), \dots, F(\Phi_{-(s-1)\delta t} a))$$

- Variable-bandwidth kernel

$$K_{\epsilon, s} : M \times M \rightarrow \mathbb{R}_+, \quad K_{\epsilon, s}(a_i, a_j) = \exp \left(- \frac{\|X_i - X_j\|^2}{\epsilon \hat{\sigma}_{\epsilon, s}^{-1/m}(X_i) \hat{\sigma}_{\epsilon, s}^{-1/m}(X_j)} \right)$$

- Diffusion maps normalization

$$\tilde{K}_{\epsilon, s} = \frac{K_{\epsilon, s}(a_i, a_j)}{\sum_k K_{\epsilon, s}(a_j, a_k)}, \quad P_{\epsilon, s}(a_i, a_j) = \frac{\tilde{K}_{\epsilon, s}(a_i, a_j)}{\sum_k \tilde{K}_{\epsilon, s}(a_i, a_k)}$$

Galerkin method for the Koopman eigenvalue problem

- We eliminate rough eigenfunctions by solving the eigenvalue problem for $L_\epsilon = v + \epsilon\Delta$

Continuous problem. Find $z \in H^1(M, h)$ and $\lambda \in \mathbb{C}$ s.t.

$$\langle \psi, v(z) \rangle + \epsilon \langle \text{grad}_h \psi, \text{grad}_h z \rangle = \lambda \langle \psi, z \rangle, \quad \forall \psi \in H^1(M, h)$$

Discrete approximation

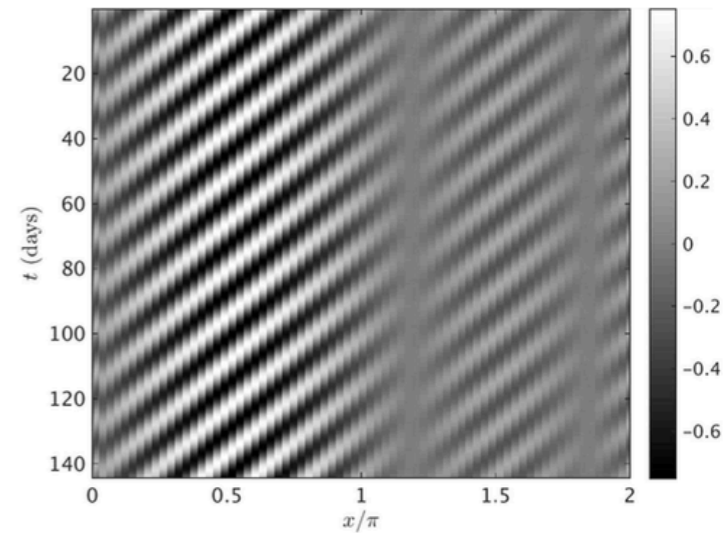
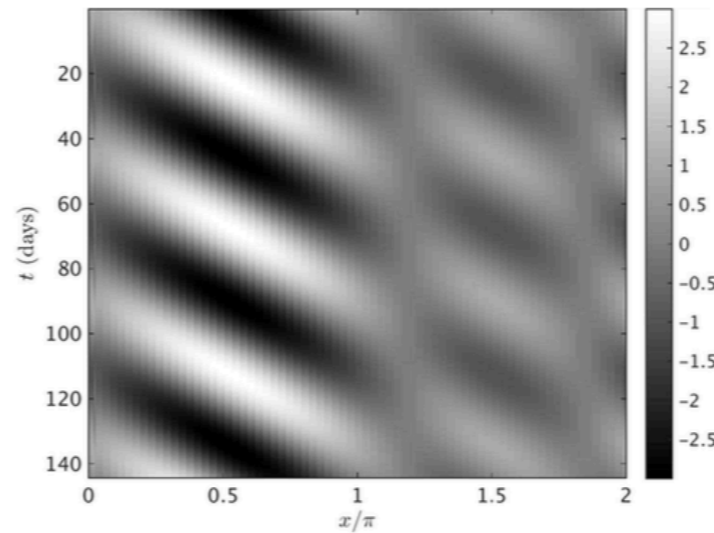
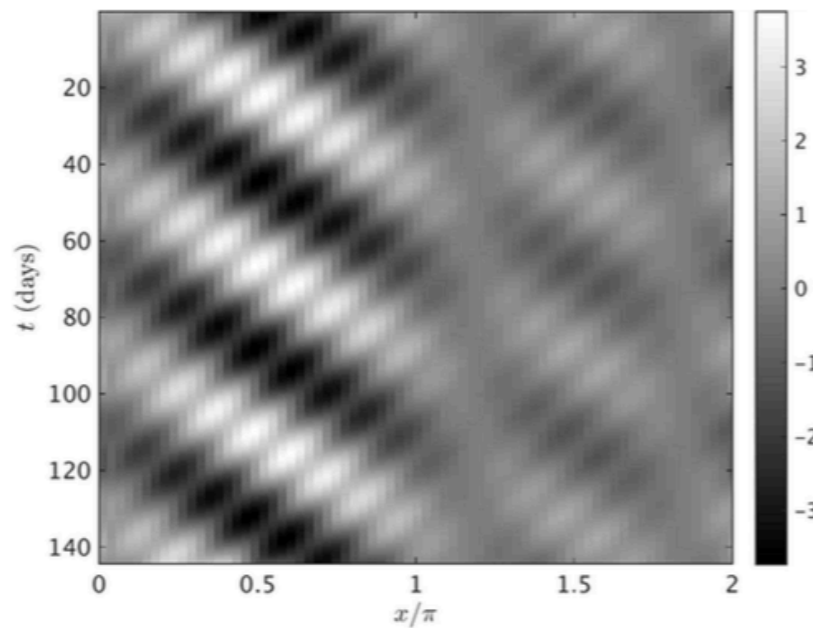
$$\sum_{j=0}^l (v_{ij} - \epsilon \delta_{ij}) c_j = \lambda \eta_i^{-1} c_i, \quad z = \sum_{i=0}^l c_i \varphi_i,$$

$$\varphi_i = \frac{\phi_i}{\eta_i^{1/2}}, \quad v_{ij} = \frac{1}{N} \sum_{k=0}^{N-1} \varphi_i(a_k) \frac{\varphi_j(a_{k+1}) - \varphi_j(a_{k-1})}{2\delta t}$$

- The action of v on functions is approximated via **finite differences** in time
- By construction of the $\{\varphi_i\}$ basis, $\langle \text{grad}_h \varphi_i, \text{grad}_h \varphi_j \rangle = \delta_{ij}$, and the scheme remains well-conditioned at large l

Traveling waves in synthetic dataset

$$u_{x,t} = (0.5 + \sin(x)) [2 \cos(k_1 x - \Theta_1(t)) + 0.5 \cos(k_2 x - \Theta_2(t))]$$



Kikuchi and Wang (2010)

$$k_1 = 2, k_2 = 10$$

$$\Theta_i(t) = \omega_i t$$

$$\omega_1 = \frac{2\pi}{45}, \omega_2 = \sqrt{10}\omega_1$$

Reconstructed
data

Diffusion maps and Koopman eigenfunctions

In systems with pure point spectra of the Koopman operators, $\bar{\Delta}f = \lim_{s \rightarrow \infty} \Delta_s f$ is well defined, and $[\bar{\Delta}, v] = 0$ (Giannakis 2015)

Eigenfunctions of $\bar{\Delta}$ provide an efficient approximation space for eigenfunctions of v

Timescale separation

Eigenfunctions recovered by diffusion maps with delays embeddings have timescale separation (Giannakis & Majda 2012, Berry et al. 2013)

Removing i.i.d. measurement noise

For data $\tilde{x}_i = x_i + \xi_i$, $x_i = F(a_i)$, corrupted by i.i.d. noise ξ_i ,

$$\mathbb{E}\|\tilde{x}_i - \tilde{x}_j\|^2 = \|x_i - x_j\|^2 + 2R^2, \quad R^2 = \text{var } \xi_i$$

Performing delay-coordinate maps, and taking the limit $s \rightarrow \infty$,

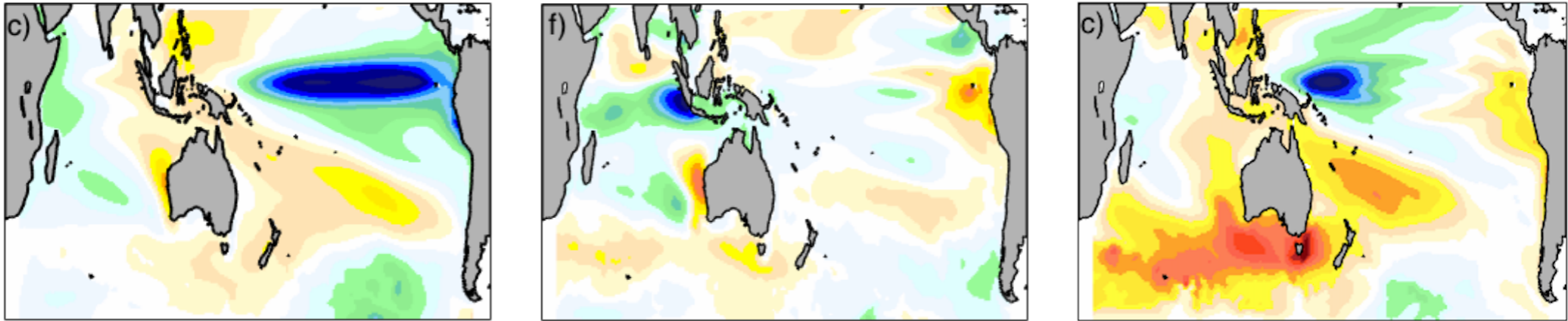
- $\|\tilde{X}_i - \tilde{X}_j\|^2 \xrightarrow{\text{a.s.}} \|X_i - X_j\|^2 + 2R^2$
- Because \bar{g} is flat, the bias term in the pairwise distance produces a multiplicative bias in the kernel which cancels to $O(\epsilon^2)$ in the **diffusion maps normalization**

$$\tilde{K}_\epsilon(a_i, a_j) = \exp\left(-\frac{\|\tilde{X}_i - \tilde{X}_j\|^2}{\epsilon \sigma_{s,\epsilon}^{-1/m}(\tilde{X}_i) \sigma_{s,\epsilon}^{-1/m}(\tilde{X}_j)}\right) \rightarrow e^{-\frac{2R^2}{\epsilon(C^2 + O(\epsilon^2))}} K_\epsilon(a_i, a_j),$$

$$\sum_j \tilde{P}_\epsilon(a_i, a_j) f(a_j) = \sum_j \frac{\frac{\tilde{K}_\epsilon(a_i, a_j)}{\sum_k \tilde{K}_\epsilon(a_j, a_k)}}{\sum_l \frac{\tilde{K}_\epsilon(a_i, a_l)}{\sum_k \tilde{K}_\epsilon(a_l, a_k)}} f(a_j) \rightarrow \int_M P_\epsilon(a_i, b) f(b) d\mu + O(\epsilon^2)$$

- Since $\int_M P_\epsilon(a_i, b) f(b) d\mu = f(a_i) - \epsilon \Delta_{\bar{g}} f(a_i) + O(\epsilon^2)$, this bias does not affect the convergence of the eigenfunctions of P_ϵ to the eigenfunctions ϕ_k of $\Delta_{\bar{g}}$ as $\epsilon \rightarrow 0$, and the denoised ϕ_k can be employed in the Galerkin scheme for Koopman eigenfunctions

Indo-Pacific SST datasets



CCSM4 control

1300 y monthly-averaged SST, 1° (nominal), preindustrial forcings

GFDL CM3 control

800 y monthly-averaged SST, 1° (nominal), preindustrial forcings

HadISST

Industrial era (1870–2013) SST, 1°

Satellite era (1979–2013) SST, 1°

- No bandpass filtering or detrending performed
- Results checked for robustness against embedding windows 4–30 y, changes in spatial domain, addition of observational noise

Indo-Pacific SST modes recovered by NLSA

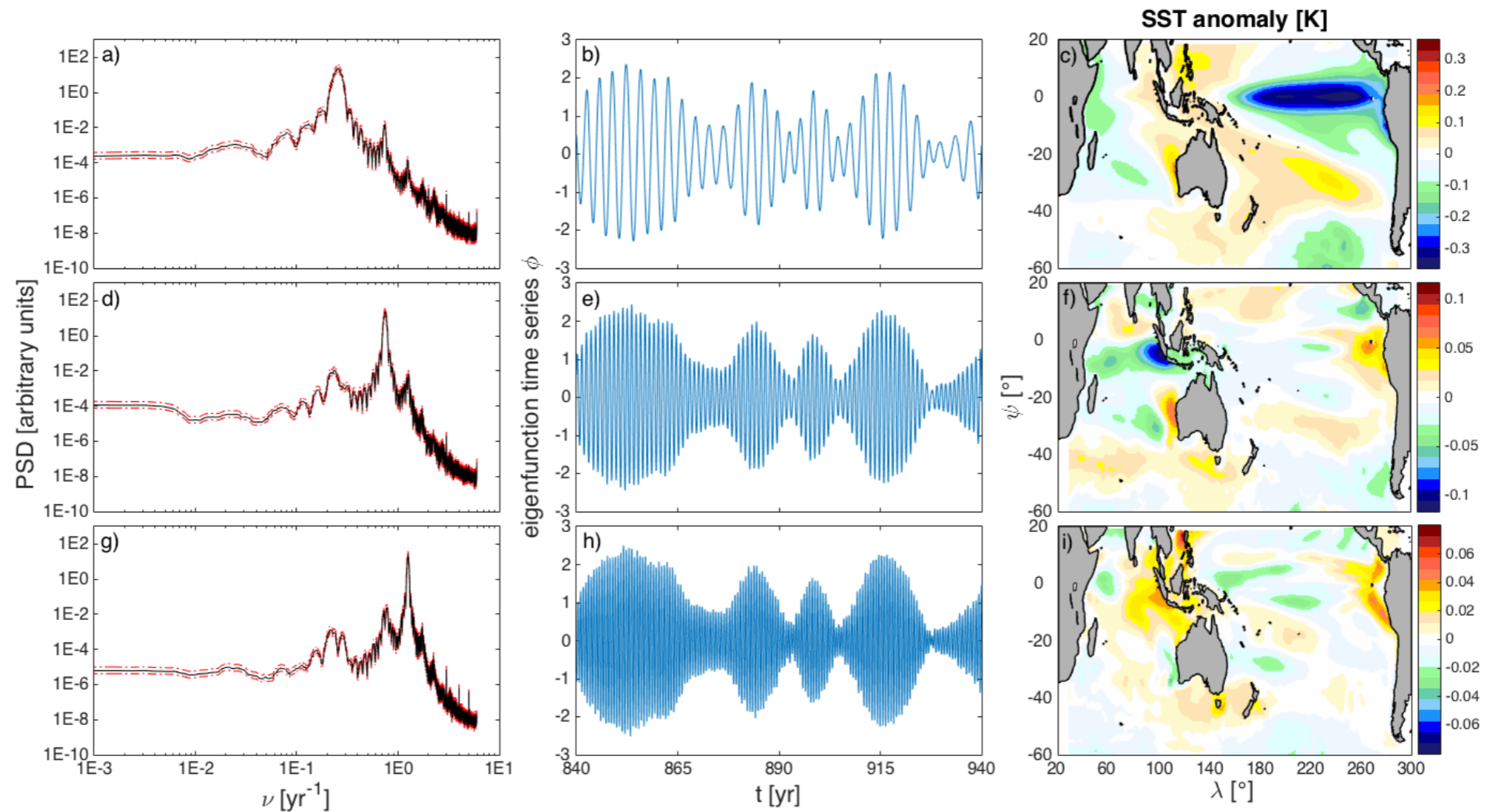
Modes from CCSM4 and CM3:

- ① Annual cycle and its harmonics
- ② ENSO and ENSO combination modes (McGregor et al. 2012; Stuecker et al. 2013; Ren et al. 2016)
- ③ Tropospheric biennial oscillation (TBO) (Meehl 1987) and associated combination modes
- ④ Interdecadal Pacific oscillation (IPO) (Power et al. 1999)
- ⑤ West Pacific multidecadal mode (WPMM)

Modes from HadISST:

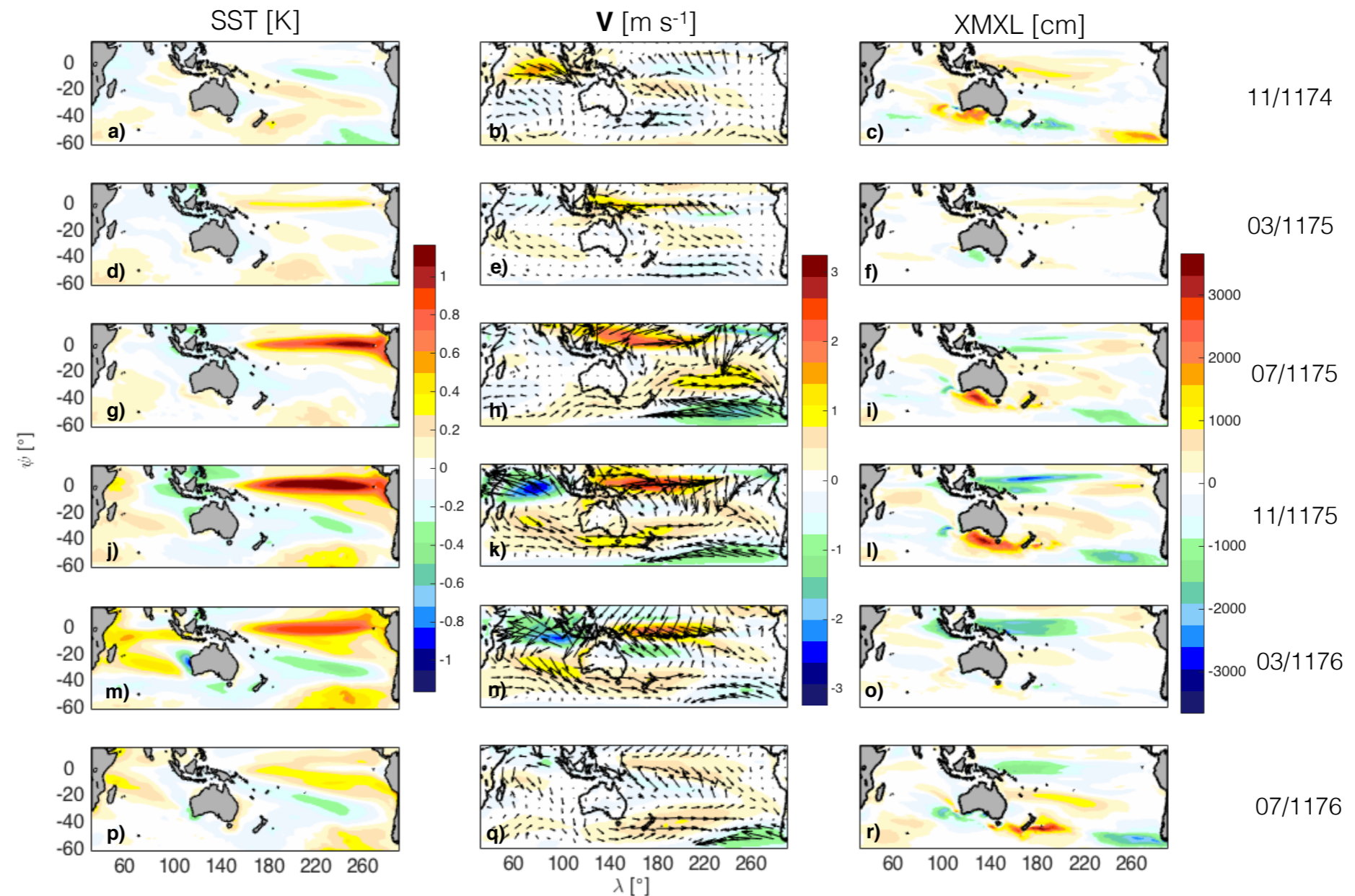
- Annual, ENSO, and TBO modes robustly recovered
- Evidence for IPO and WPMM (though of degraded quality)

ENSO and ENSO combination modes



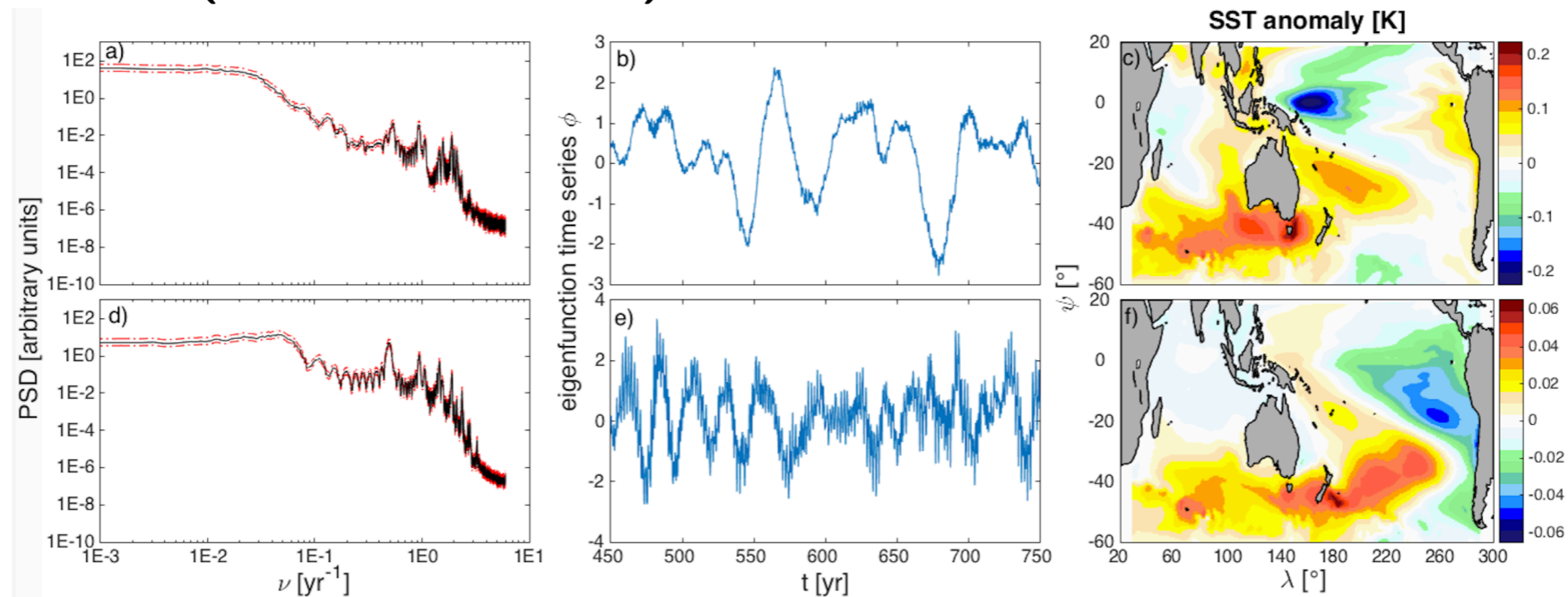
- ENSO emerges as an oscillatory pair of eigenfunctions with a $\nu_{\text{ENSO}} \approx 4 \text{ y}^{-1}$ frequency peak and a **decadal amplitude envelope**
- **Combination modes** predicted from quadratic nonlinearities in the coupled atmosphere-ocean system (McGregor et al. 2012; Stuecker et al. 2013) are recovered at the theoretically expected frequencies $\nu_{\text{ENSO}} \pm 1 \text{ y}^{-1}$ and degeneracies
- The ENSO and ENSO combination modes together capture the phase-locking of ENSO to the annual cycle

ENSO and ENSO combination modes

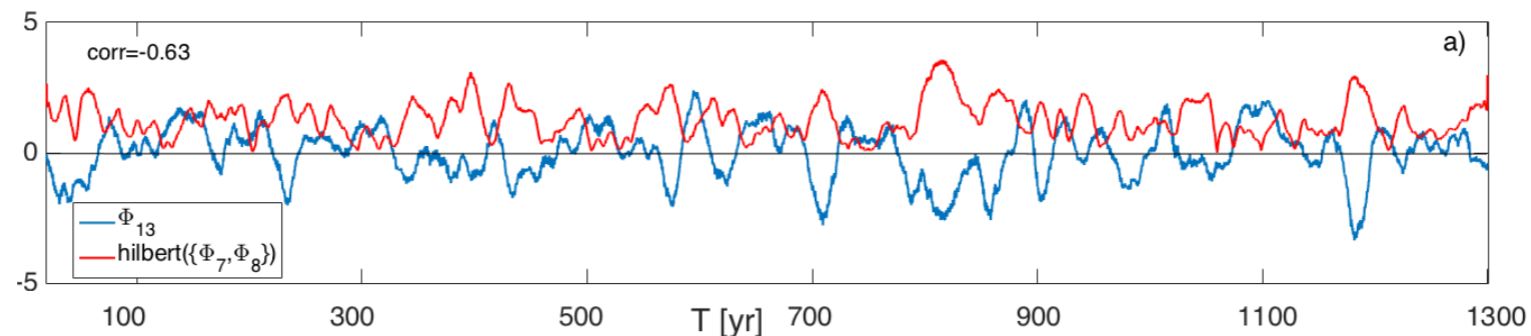


- Reconstructed surface winds exhibit **anomalous westerlies** during the development of El Niño events in boreal winter, and a **southward shift** preceding El Niño decay in boreal spring (Vecchi 2006; Stuecker et al. 2013)
- Surface circulation consistent with **Indian Ocean SST dipole** (Saji et al. 1999; Webster et al. 1999)

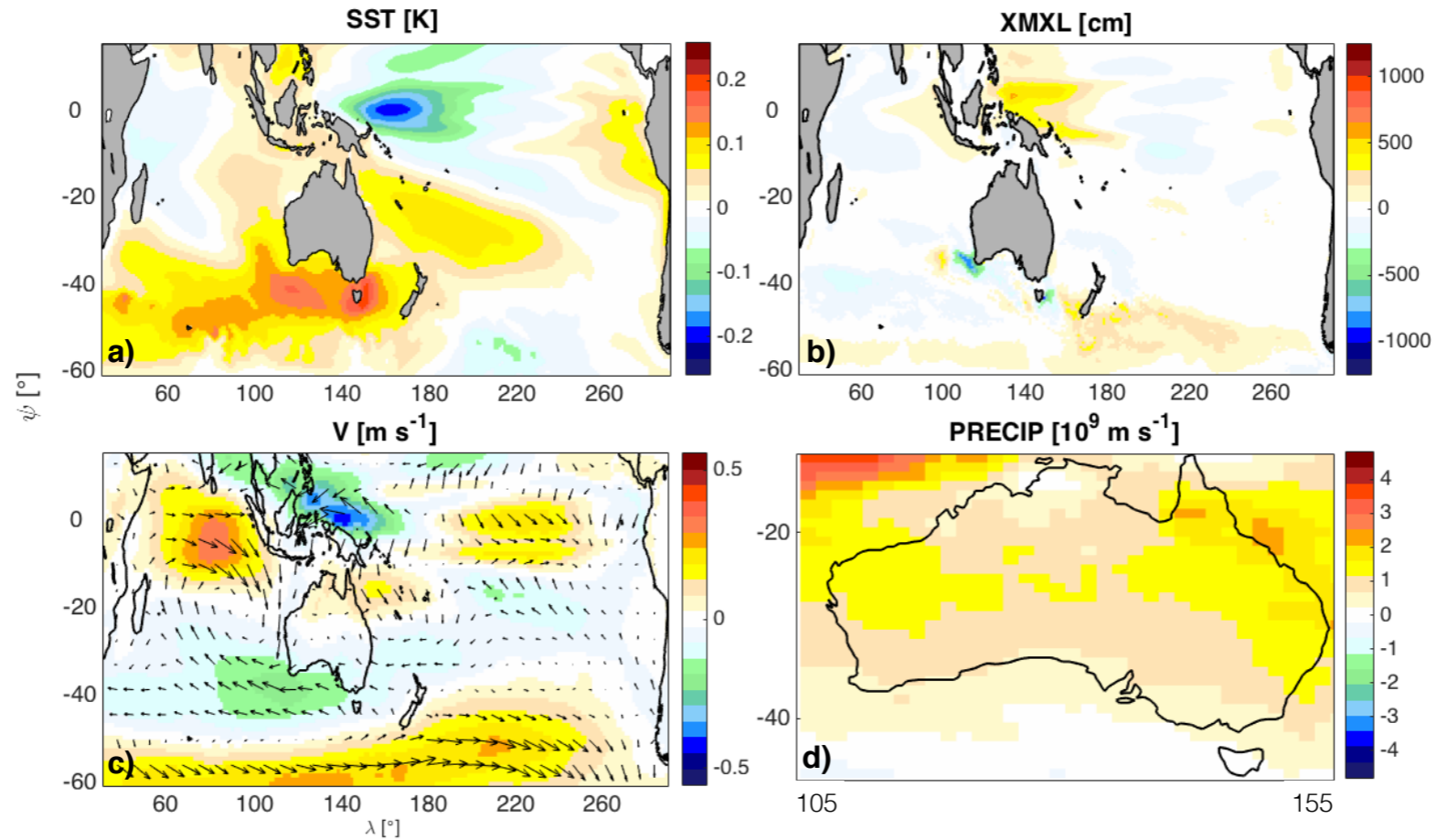
Decadal modes (WPMM & IPO)



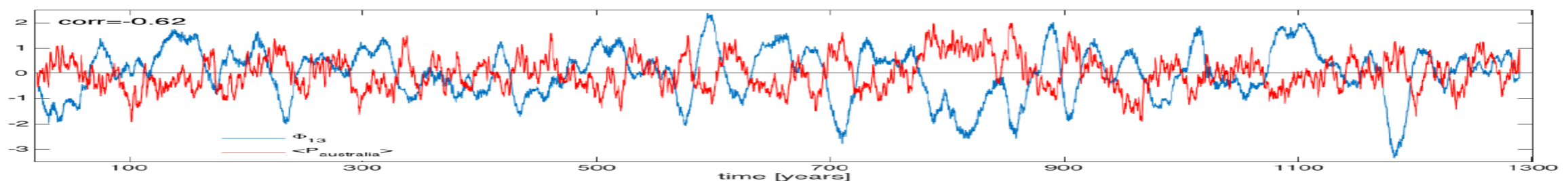
- West Pacific multidecadal mode (top) characterized by multidecadal variability and a prominent cluster of SST anomalies in the **western equatorial Pacific**
- Some similarities with 2nd EOF of decadal Pacific SST (Timmermann 2003; Ogata et al. 2013) and SST residuals (Karnauskas et al. 2009; Solomon & Newman 2012; Seager et al. 2015)
- Cold (warm) WPMM phases correlate with enhanced (suppressed) ENSO activity (corr. coeff. 0.63 in CCSM4)



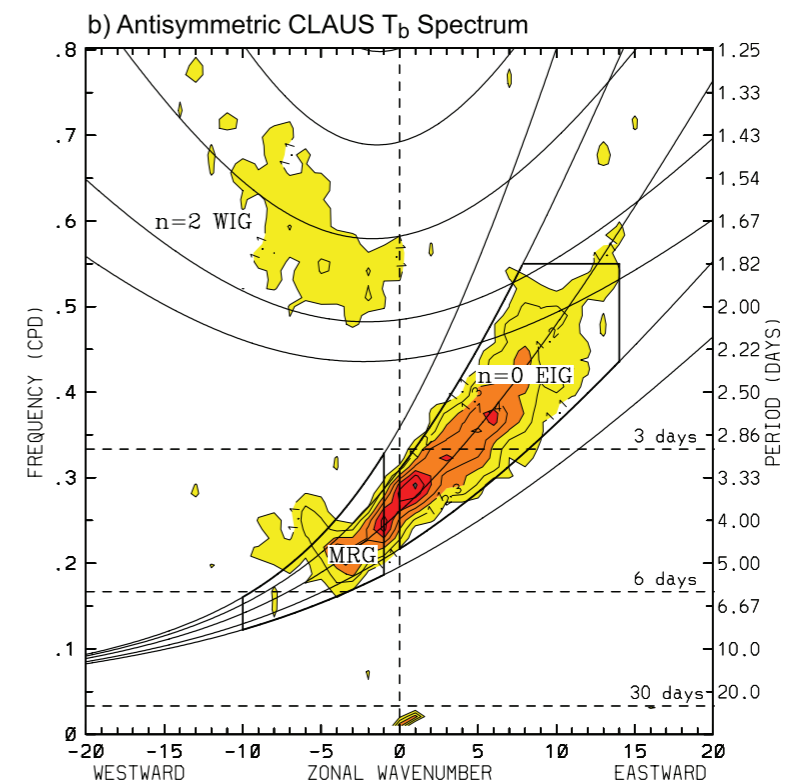
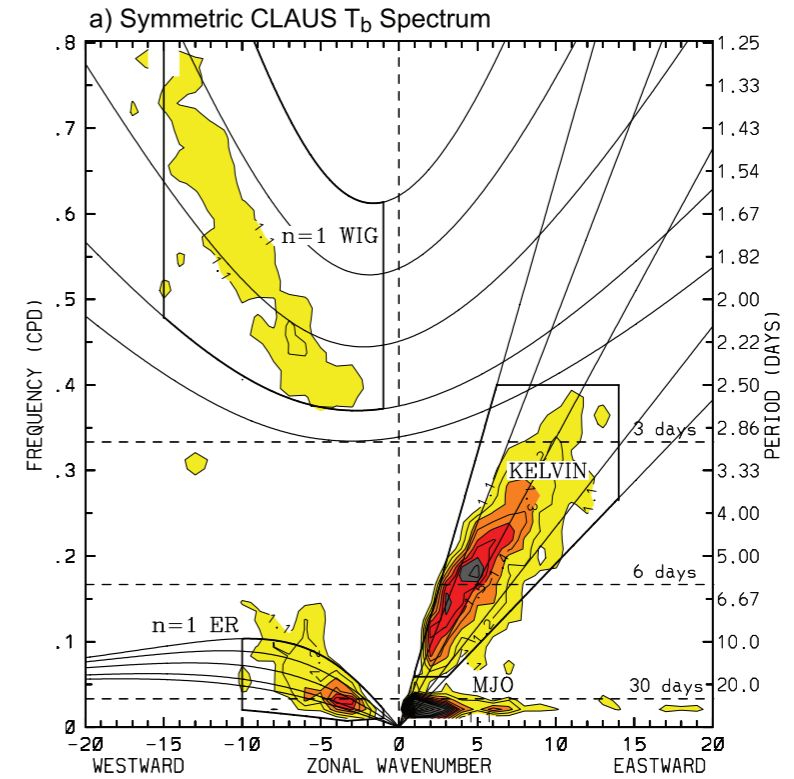
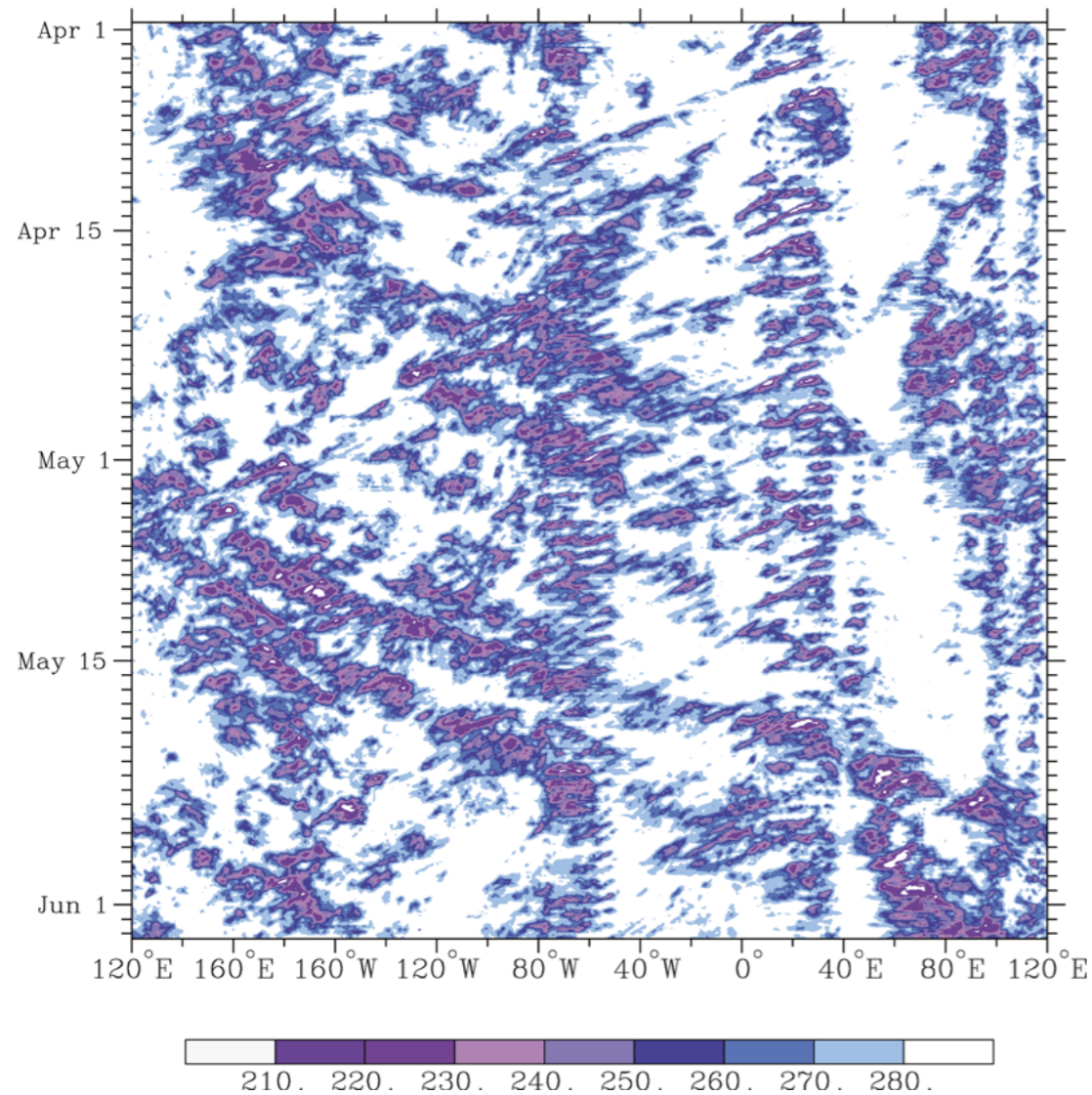
West Pacific multidecadal mode – climate impacts



- Cold WPMM phase is characterized by **anomalous westerlies in the central Pacific** and **anomalously flat zonal thermocline profile**; such conditions are known to correlate with enhanced ENSO activity (Kirtman & Schopf 1998; Kleeman et al. 1999; Fedorov & Philander 2000)
- Circulation and SST patterns are consistent with strong impacts on Australian decadal precipitation (corr. coeff. 0.62 in CCSM4)



Analysis of organized tropical convection

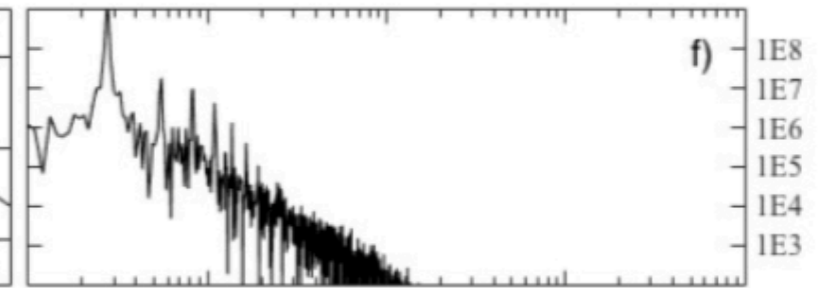
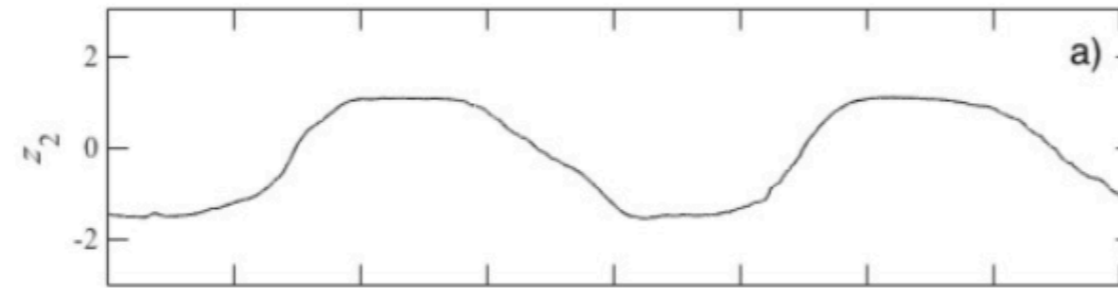


Source: Kiladis et al. (2009)

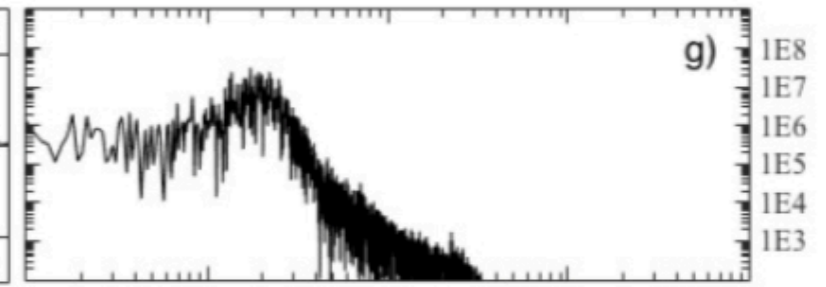
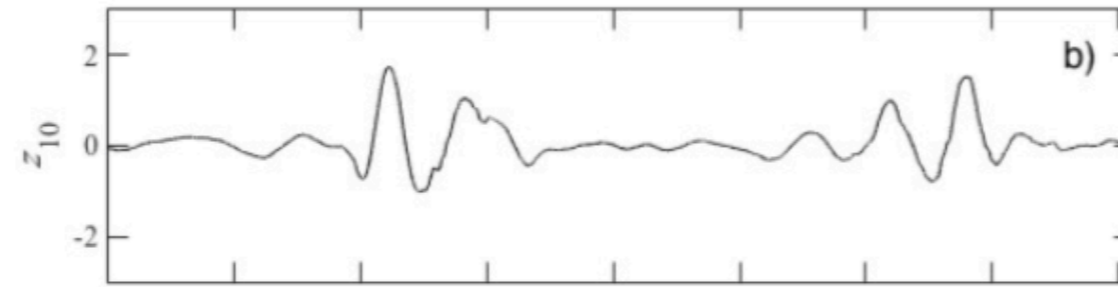
T_b from 1983-2009 CLAUS archive
 $s=512$ delays

Koopman Eigenfunctions

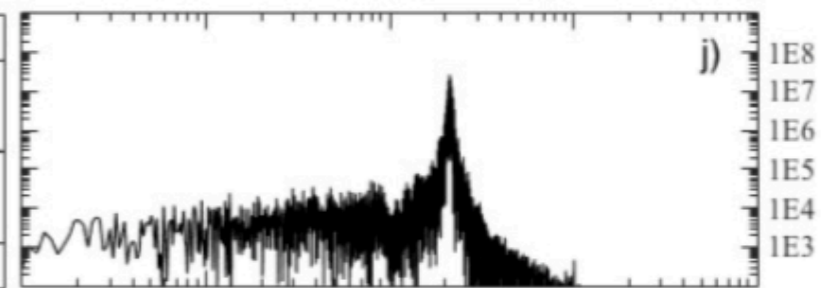
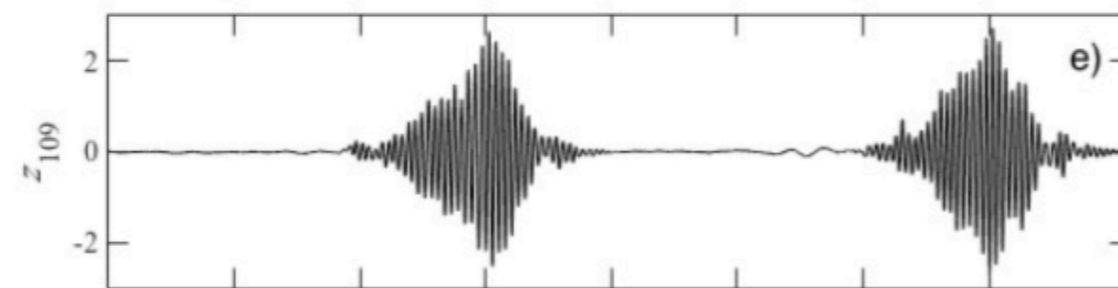
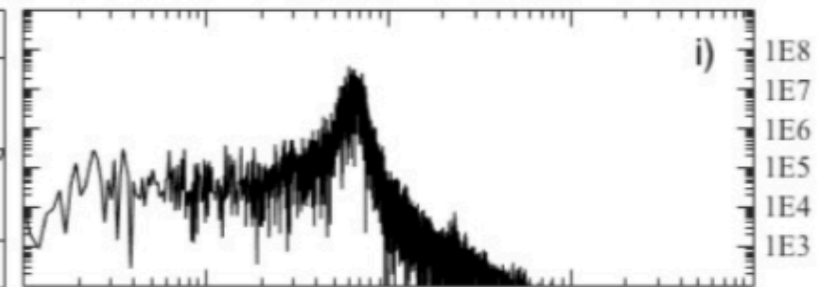
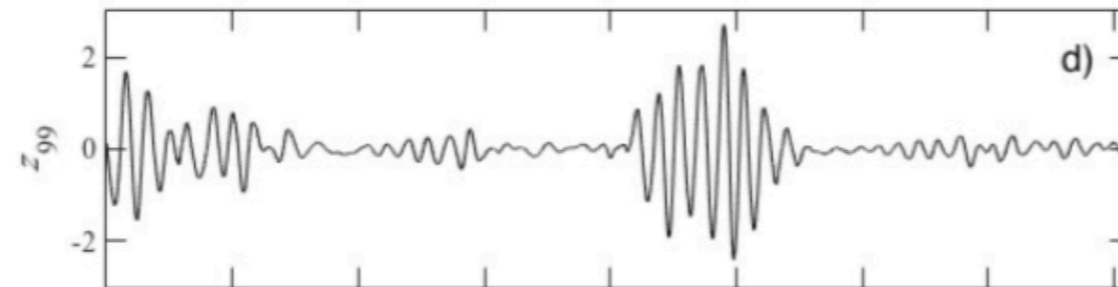
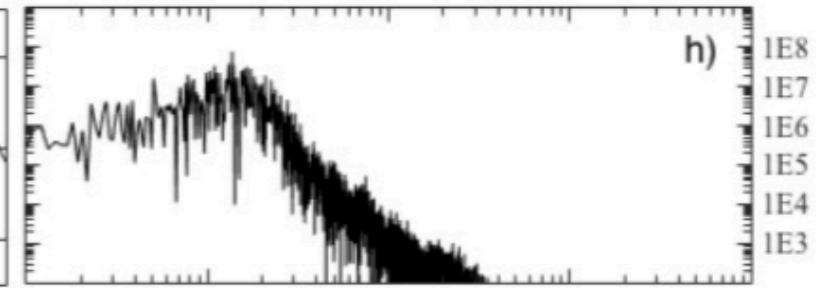
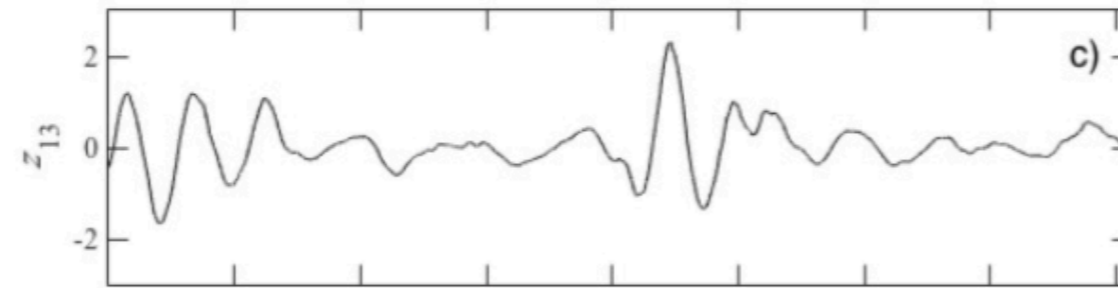
Annual cycle



Dominant intraseasonal oscillations

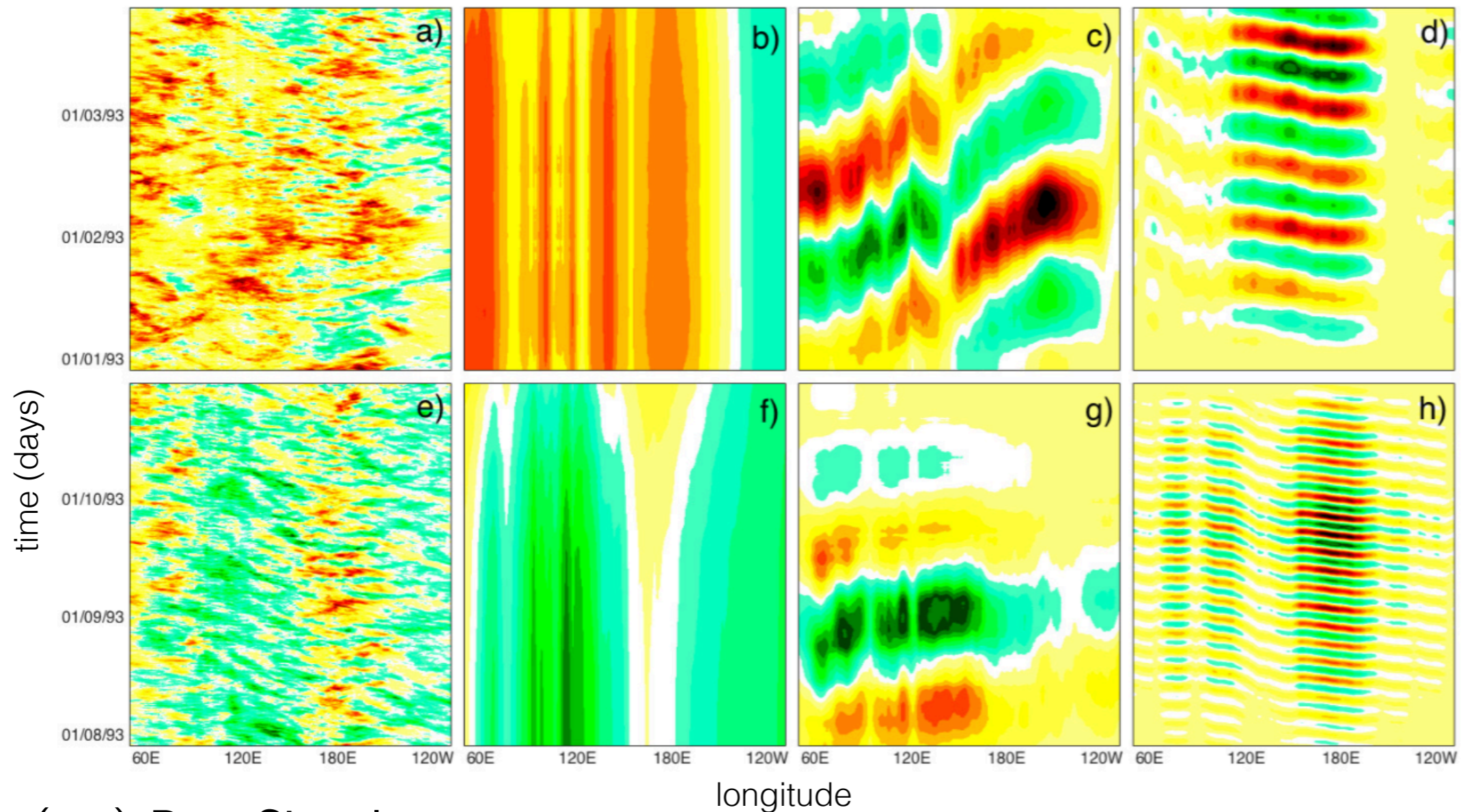


Convectively Coupled Equatorial Waves (CCEWs)



date (yymm) frequency (d^{-1})

Spatiotemporal reconstruction



(a,e) Raw Signal

(b,f) Annual cycle

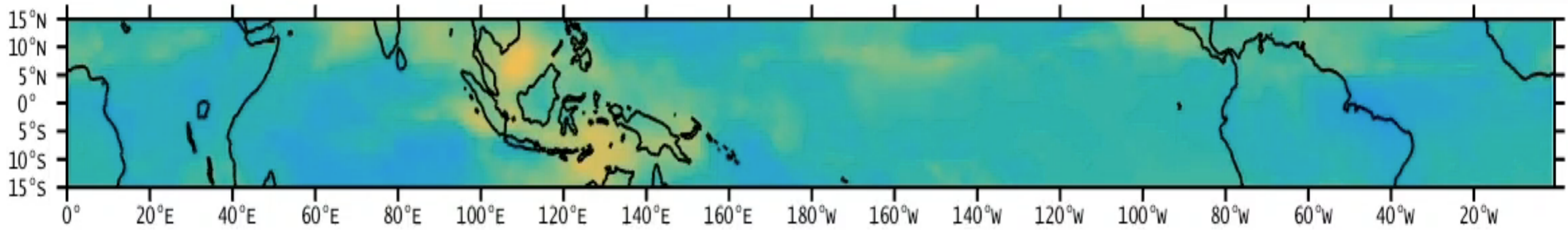
(c) Madden-Julian Oscillation (MJO)

(d,h) Westward-propagating disturbances

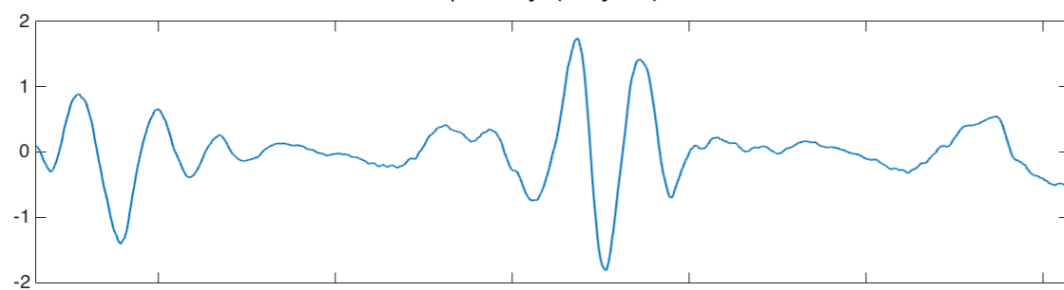
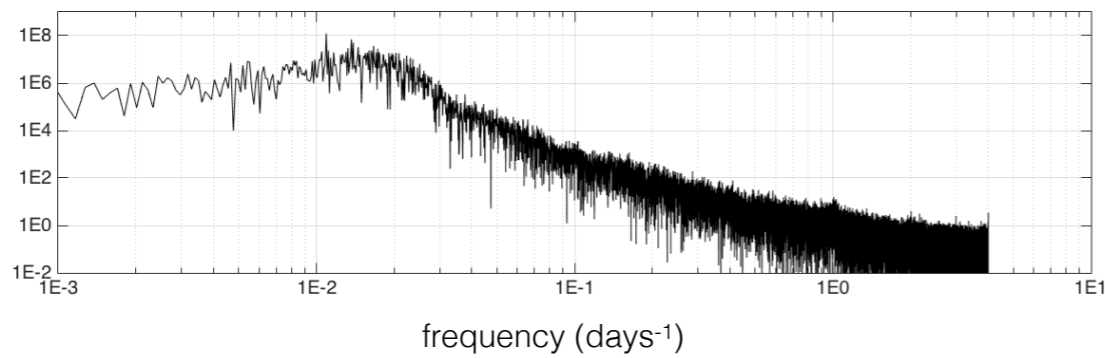
(g) Boreal Summer Intraseasonal Oscillation (BSISO)

MJO

lag 63 d 21 h



Temporal pattern and frequency spectrum

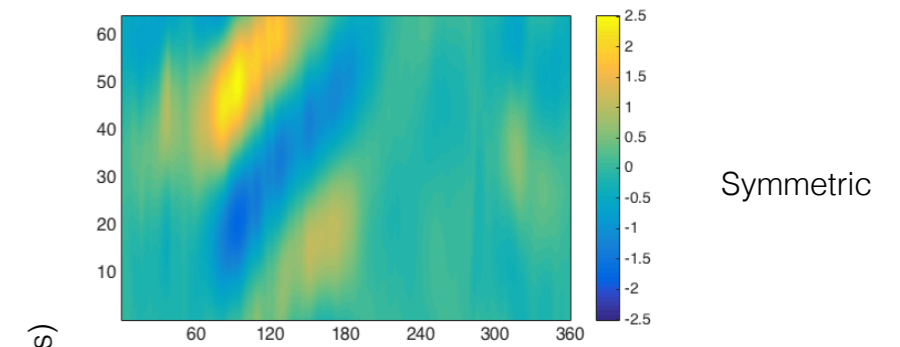


01/01/92

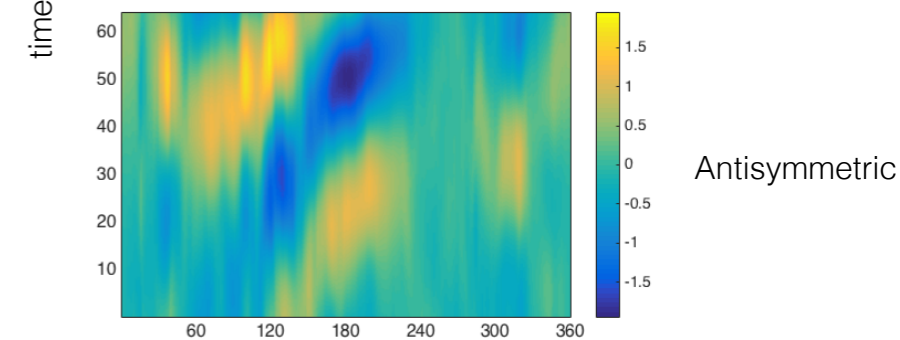
time

01/01/94

Hovmoller diagram

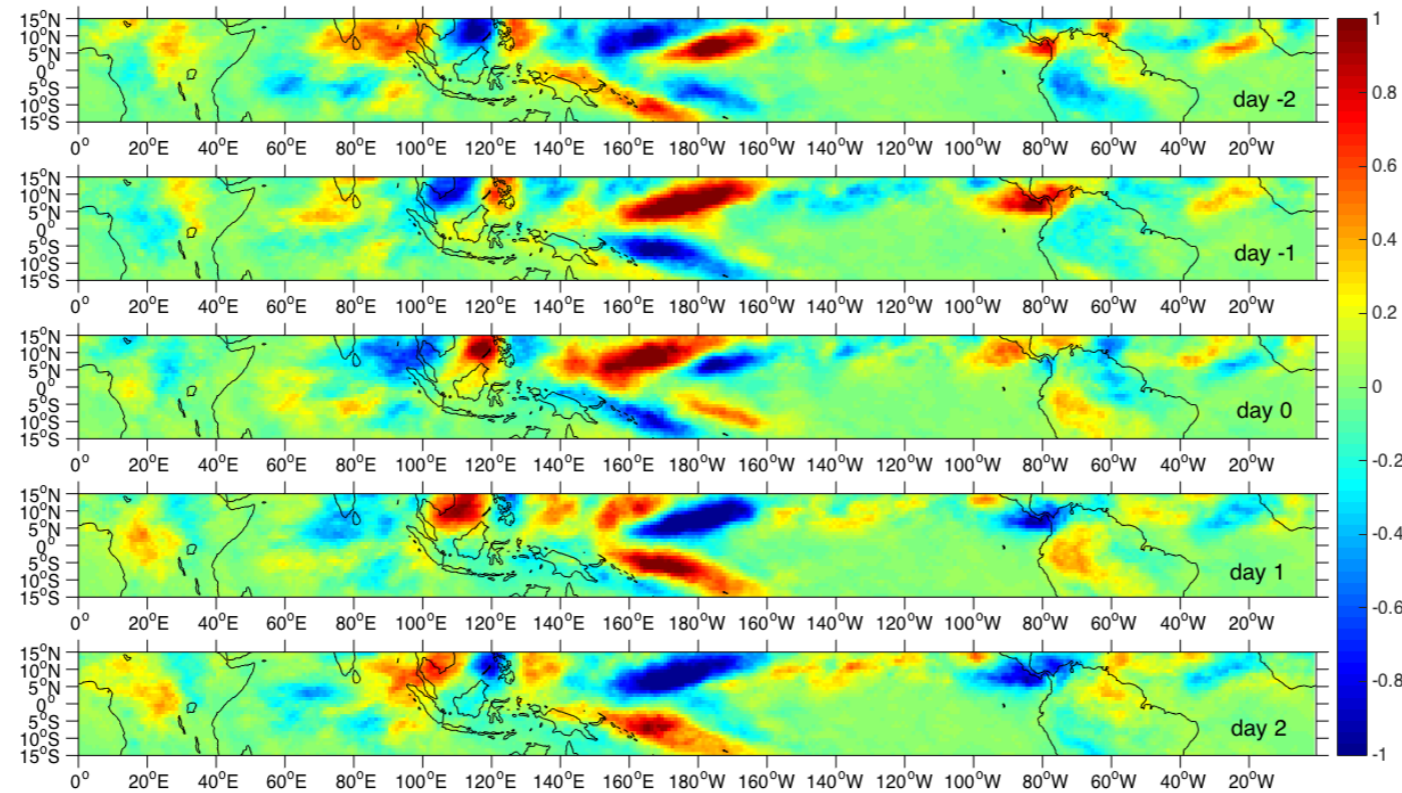


time (days)



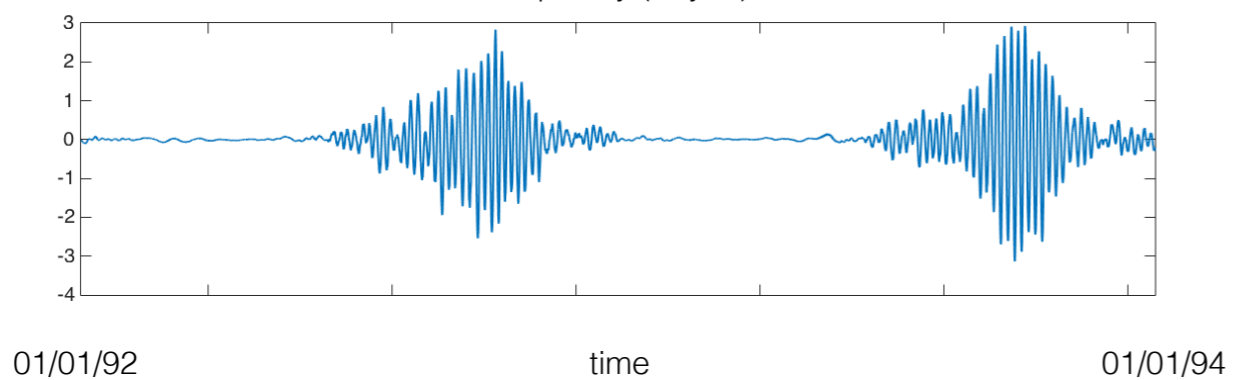
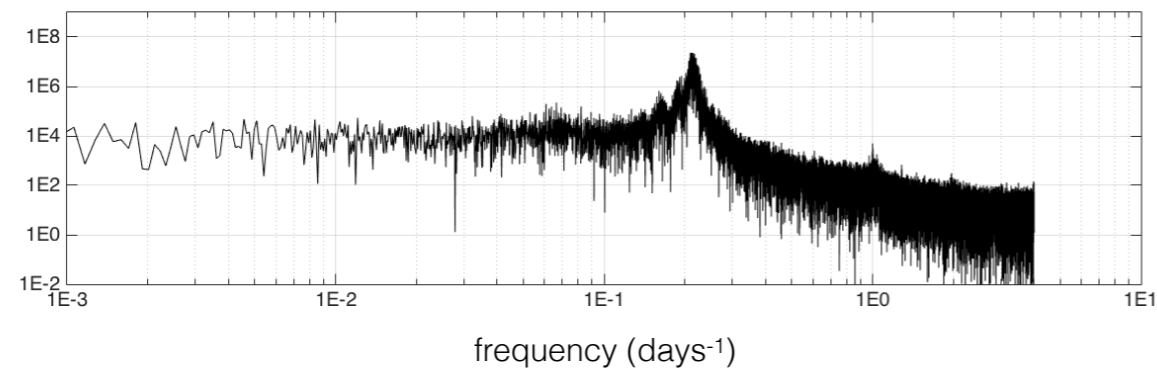
longitude

CCEW: mixed Rossby-gravity wave

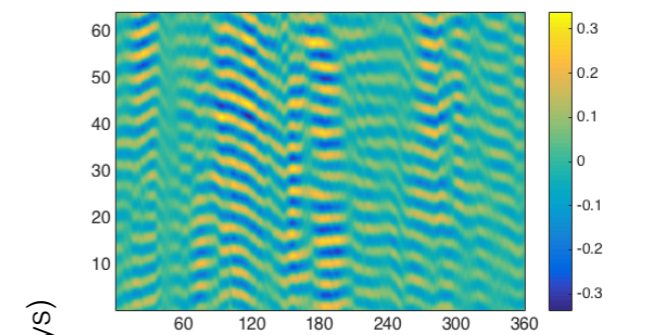


lag 63 d 21 h

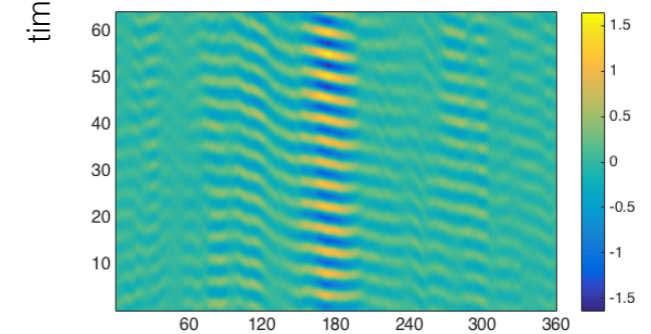
Temporal pattern and frequency spectrum



Hovmoller diagram

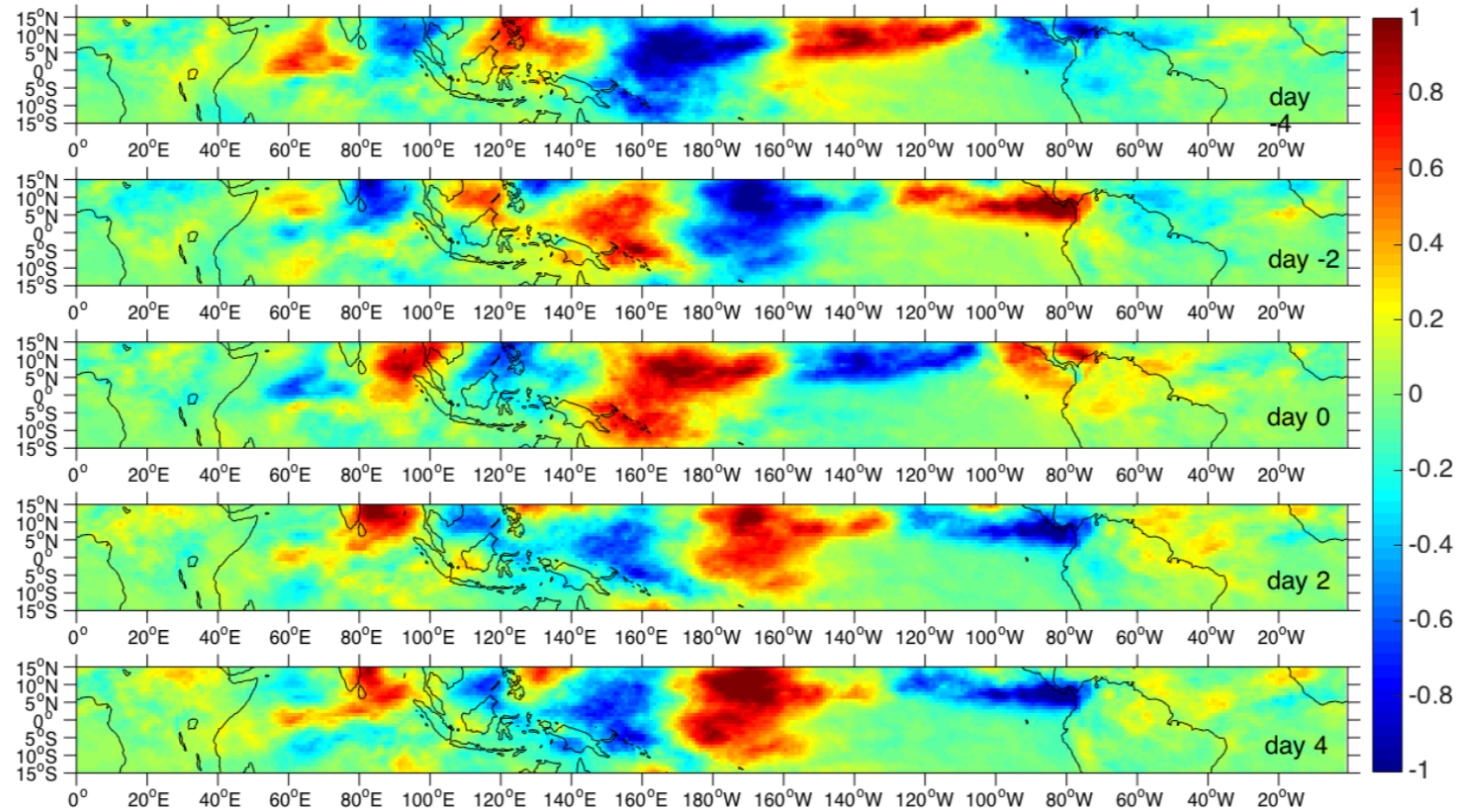


Symmetric



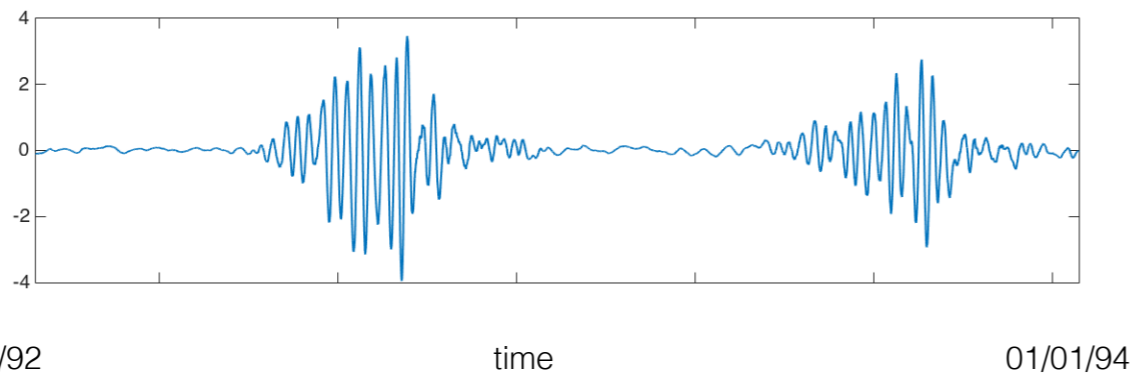
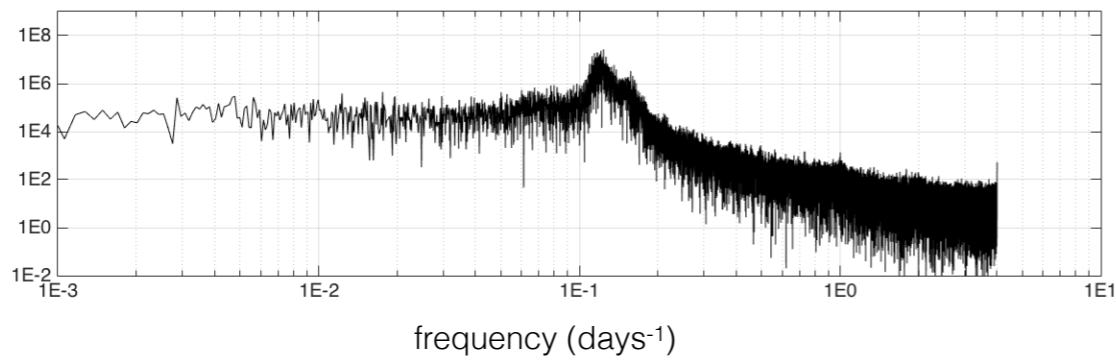
Antisymmetric

CCEW: Kelvin wave

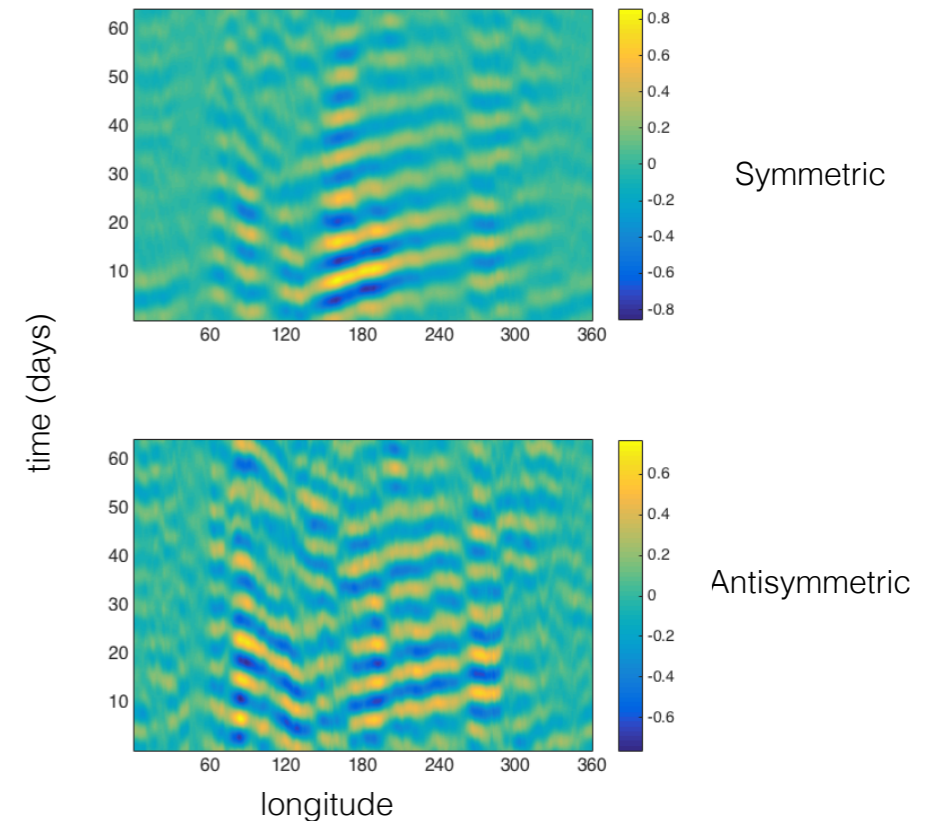


lag 63 d 21 h

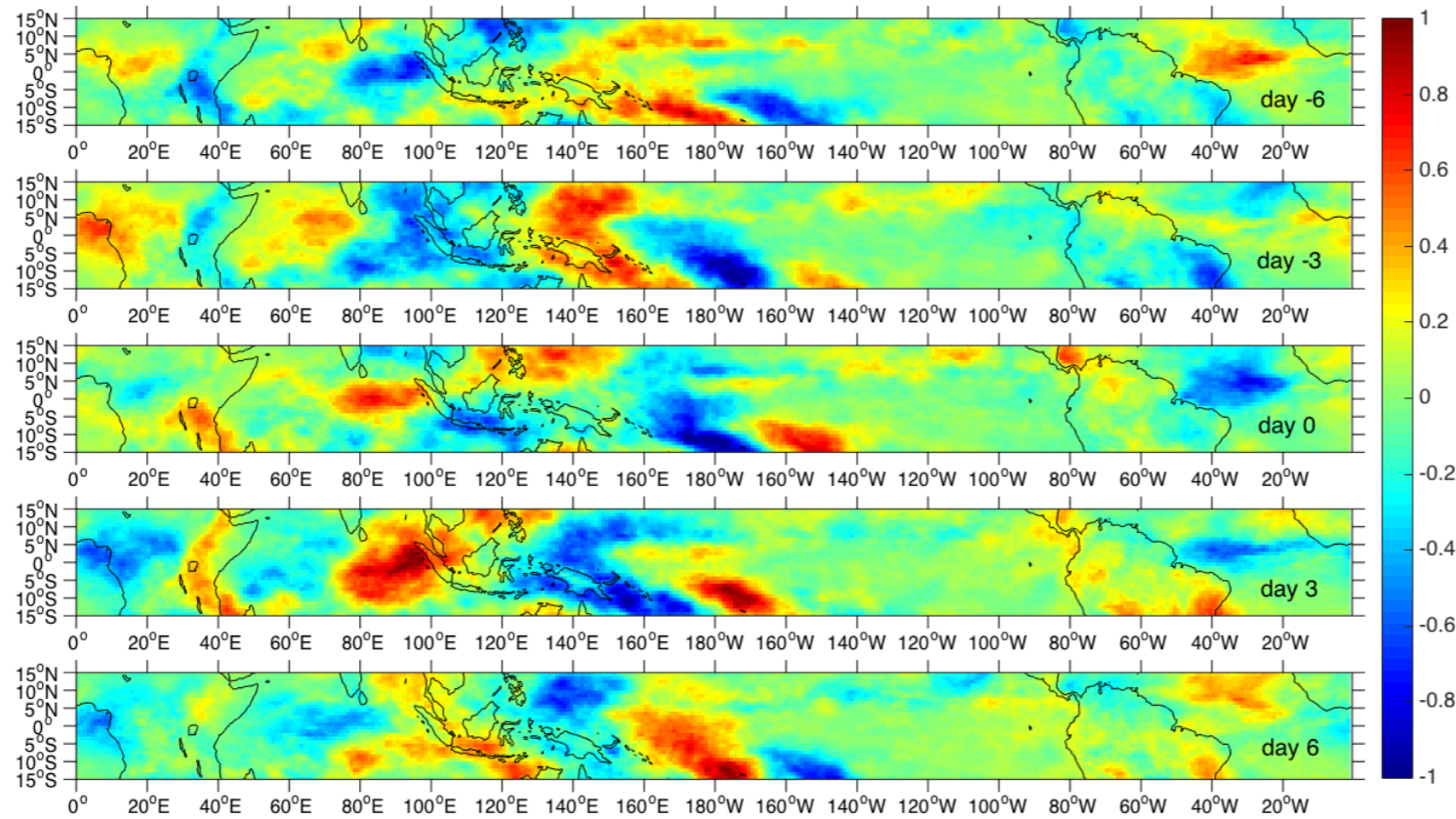
Temporal pattern and frequency spectrum



Hovmoller diagram

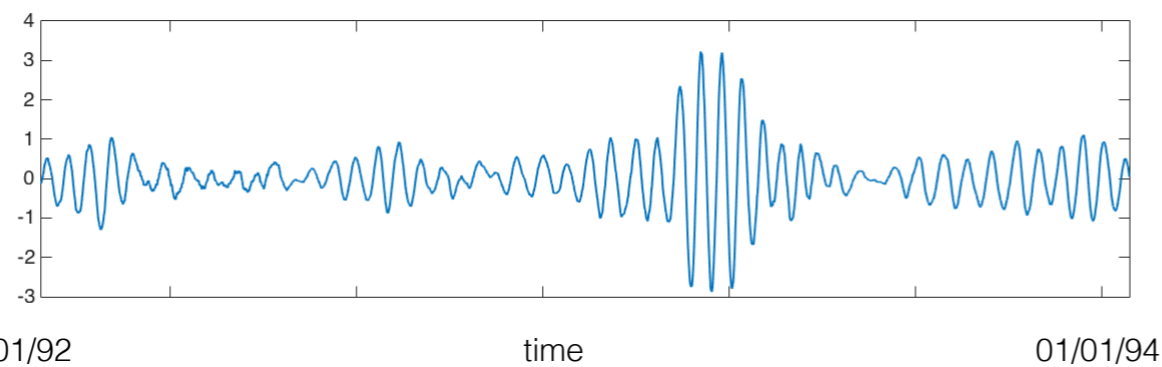
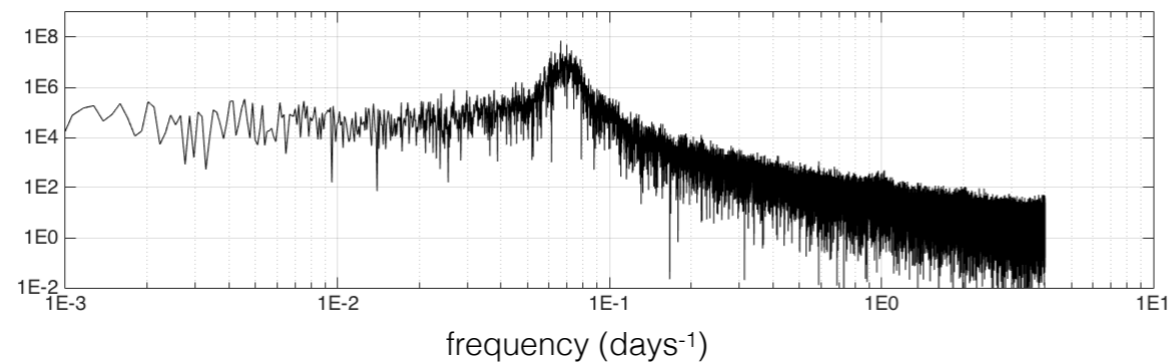


CCEW: equatorial Rossby wave

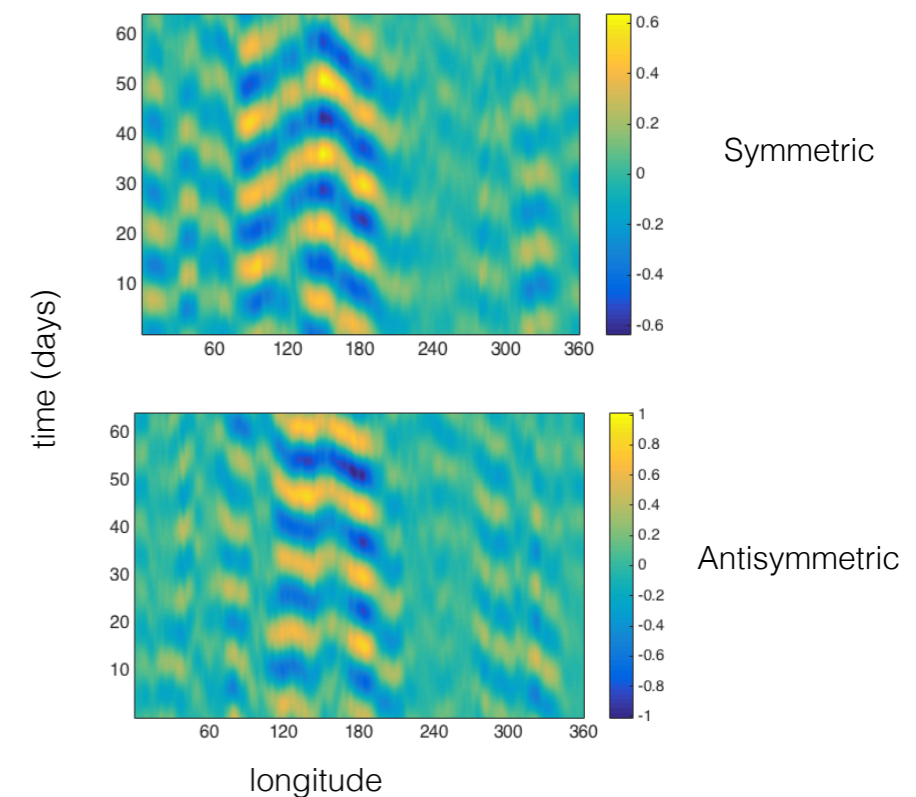


lag 63 d 21 h

Temporal pattern and frequency spectrum



Hovmoller diagram



Summary

- We have demonstrated the potential of data-driven Koopman operator techniques for extraction of spatiotemporal patterns from high-dimensional multiscale timeseries generated by nonlinear dynamical systems.
- The method relies on constructing low-dimensional representations (feature maps) of spatiotemporal signals using eigenfunctions of the Koopman operator governing the evolution of observables in ergodic dynamical systems.
- This operator is estimated from time-ordered data through a Galerkin scheme applied to basis functions computed via the diffusion maps algorithm.
- In particular, applying this method to 2D brightness temperature data over the tropics, we identified several propagating patterns corresponding to CCEWs.
- To our knowledge, recovery of such patterns from brightness temperature data has previously not been possible via objective eigendecomposition techniques.

References

- D. Giannakis and A. J. Majda (2012), Nonlinear Laplacian spectral analysis for time series with intermittency and low-frequency variability. *Proc. Natl. Acad. Sci.*, 109(7),2222-2229
- D. Giannakis (2015), Data-driven Spectral Decomposition and Forecasting of Ergodic Dynamical Systems. [arXiv:1507.02338](https://arxiv.org/abs/1507.02338)
- D. Giannakis, J. Slawinska, and Z. Zhao (2015), Spatiotemporal Feature Extraction with Data-Driven Koopman Operators. *J. Mach. Learn. Res. Workshop and Conference Proceedings*, 44
- J. Slawinska and D. Giannakis (2016), Spatiotemporal pattern extraction with data-driven Koopman Operators for Convectively Coupled Equatorial Waves. *Proceedings for 6th International Climate Informatics Workshop*
- J. Slawinska and D. Giannakis (2016), Indo-Pacific Variability on Seasonal to Multidecadal Timescales. Part I: Intrinsic SST Modes in Models and Observations. *J. Climate*, in revision
- D. Giannakis and J. Slawinska (2016), Indo-Pacific Variability on Seasonal to Multidecadal Timescales. Part II: Multi-Scale Ocean–Atmosphere Interactions. *J. Climate*, in revision